26 July 2022

CFACT 2022
Radiosonde Data Quality Report

Holger Vömel, William Brown
Earth Observing Laboratory
National Center for Atmospheric Research
Boulder, CO

Earth Observing Laboratory
In situ Sensing Facility

NATIONAL CENTER FOR ATMOSPHERIC RESEARCH
P. O. Box 3000
BOULDER, COLORADO 80307-3000

The radiosonde data for this project were quality controlled and are maintained by the Earth Observing Laboratory at the National Center for Atmospheric Research (NCAR). The National Center for Atmospheric Research is managed by the University Corporation for Atmospheric Research and sponsored by the National Science Foundation.

If information or plots from this document are used for publication or presentation purposes, please provide appropriate acknowledgement to NCAR/EOL and NSF and refer to the citation listed below. Please feel free to contact the authors for further information.

Contacts:

Holger Vömel (voemel@ucar.edu)
Bill Brown (wbrown@ucar.edu)

Radiosonde operators:

NCAR: Bill Brown, Isabel Suhr, John Sobtzak, Liz Bernhardt, Lou Verstraete, Matt Paulus, Steve Oncley, Jacquie Witte

U. Utah: Bayasal Baterdene, Rebecca Beal, Gerardo Carrillo-Cardenas, Zac Claerhout, Jebediah Dean, Pete Gombert, Noah Hirshorn, Sebastian Hoch, Nic Hofmann, Pauline Kneller, Grace Liu, Angelina Miller, Travis Morrison, Alexi Perelet, Michael Pletcher, Zhaoxia Pu, Haley Scott, Ben Silberman, Nancy Sohlberg, Johnathan Stoddard, Michael Wasserstein, Savanna Wolvin, Miles Worthen.

Mailing Address:

NCAR/Earth Observing Laboratory
P.O. Box 3000
3090 Center Green Dr.
Boulder, CO 80301, USA

Websites:

CFACT home page:
https://www.eol.ucar.edu/field_projects/cfact
Integrated sounding system home page:
https://www.eol.ucar.edu/content/iss-operations-cfact

To refer to this data set or report, please include the following citation:

NCAR/EOL In-situ Sensing Facility, University of Utah - Department of Atmospheric Sciences. 2022. CFACT: NCAR/EOL ISS and University of Utah Radiosonde Data. Version 1.0. UCAR/NCAR - Earth Observing Laboratory. https://doi.org/10.26023/6S3T-8RV0-WD07. Accessed 26 Jul 2022.

Document Version Control

Version	Date	Author	Change Description
1.0	25 Jul 2022	H. Vömel	Initial Data Release

1 Table of Contents

2 Dataset Overview

The Cold Fog Amongst Complex Terrain (CFACT) is a field campaign that investigates cold fog formation in mountain valleys and environmental conditions in complex terrain with the latest observation technology. Its goal is to improve microphysical parameterizations and visibility algorithms used in numerical weather prediction (NWP) models and to develop data-assimilation and analysis methods for current and next-generation (e.g., sub-kilometer scale) NWP models. From 6 January to 23 February 2022, two Integrated Sounding Systems (ISS) were deployed in the Heber Valley, Utah. This document describes the quality of the data obtained from the NCAR/EOL radiosonde launches at the location of ISS2.

Campaign staff from NCAR/EOL and the University of Utah successfully launched 120 radiosondes. Soundings were launched at least daily around 23:15 UTC (16:15 local time). Intensive observation periods (IOPs) took place on 12, 17, and 20 January, and 4, 10, 13, 18, 19, and 23 February during which up to 8 radiosondes per day were launched.

Only one sounding failed shortly after launch due to a leaking balloon, requiring a re-launch. Two soundings did not provide data to the balloon ceiling due to a failure of the temperature sensor. The overall success rate of the sounding operations during this campaign was 98%.

Figure 1 shows the flight tracks of the ascending part of all soundings.

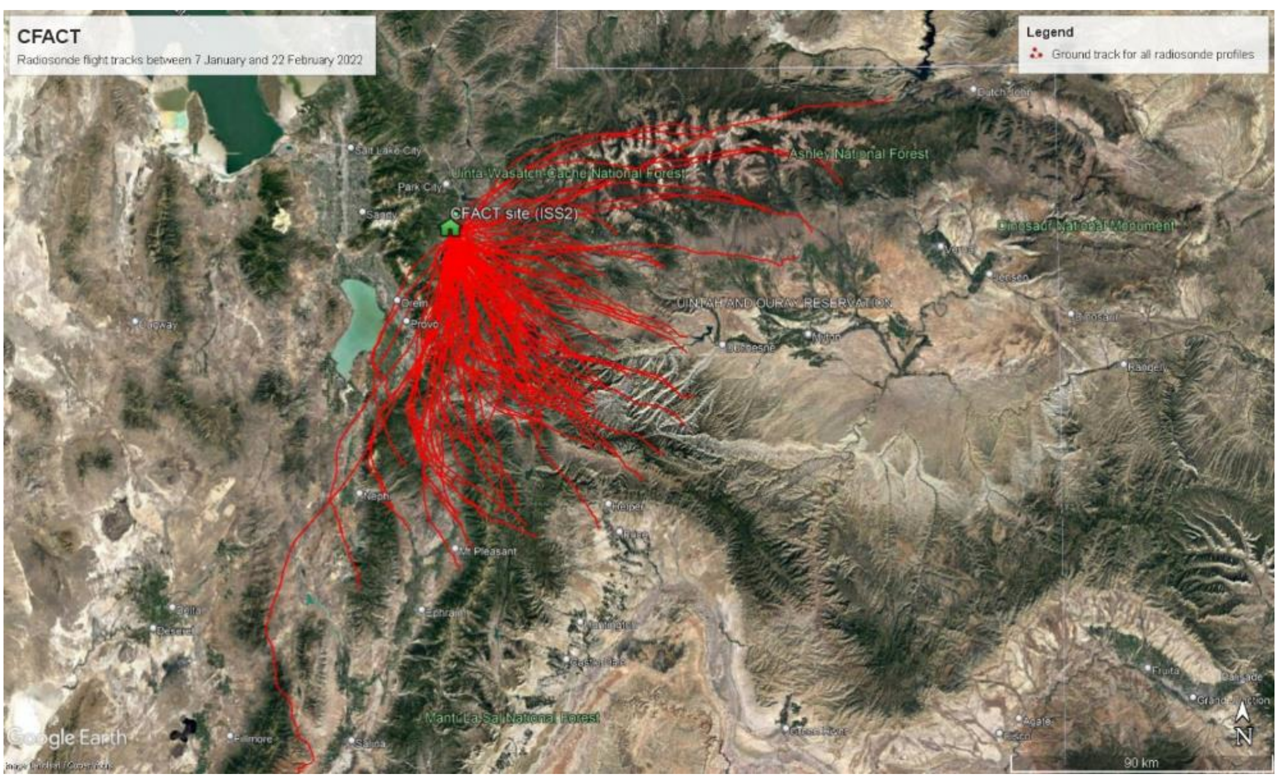

Figure 1: Location of the ISS site during CFACT and flight tracks of all ascending radiosonde profiles. The sounding location was 4.7 km west of Heber City, UT.

3 Radiosonde sounding system

This campaign used Vaisala RS41-SGP radiosondes, which were received and processed by the Vaisala MW41 sounding system using software version 2.17.0. The radiosondes used by NCAR/EOL include a pressure sensor, which provides a better altitude and pressure determination in the boundary layer and is more suitable for unstable conditions in convective environments. The sounding system was configured to meet the needs of NCAR for high-resolution data and complete metadata description. All sondes were launched using 100 g balloons supplied by Scientific Sales.

The MWX raw data files from the sounding system were saved along with the ASCII output files, which contained the initially processed profiles.

Data were recorded also on descent; however, these data are not analyzed but can be made available only upon request.

The sounding systems automatically ingests surface reference observations, which are provided by sets of reference sensors near each launch site. These observations are stored in the surface observations metadata fields of the sounding files and used in the quality control procedures of the sounding data.

The reference sensors used for the radiosonde system during CFACT are listed in Table 1.

Table 1: Surface reference observations provided by the ISS meteorological reference sensors during CFACT.

Parameter	Location	Sensor
Pressure	The reference pressure was installed on a mast at 2 m height near the launch site.	PTB220
Temperature and humidity	The reference sensors for temperature, humidity, wind speed, and wind direction were installed on a mast at 3 m height near the launch site.	Lufft WS800
Wind	The reference sensor for wind speed and wind direction was installed on a mast at 3 m height near the launch site.	Lufft WS800

4 Quality control procedures

4.1 Standard quality control

The Vaisala system performs a sequence of standard quality control procedures and corrections for all radiosonde data:

- Applies a ground check correction for pressure using the pressure correction measured during the sonde preparation to compensate for small biases inherent in this type of pressure sensor.
- Performs a coarse outlier check for all measurement parameters
- Automatically detects launch based on change in pressure
- Performs a radiation correction for the temperature measurement using the radiation correction lookup table for the Vaisala RS41 radiosonde
- Corrects for response time lag of the temperature sensor
- Smooths the temperature profile
- Corrects for response time lag of the humidity sensor
- Filters out the balloon pendulum effect in the calculation of winds
- Calculates geopotential altitude based on the measured pressure profile

4.2 Custom quality control

In addition to the standard Vaisala procedures, all metadata are verified, and all measured parameters including reference measurements are checked for consistency and for any previously unidentified issue. The radiosonde measurements before launch are compared against the reference measurements and the causes for early termination are investigated. In the CFACT data set, the following issues were identified and corrected:

a. The Vaisala system removed up to 3 seconds of data after launch due to a super-adiabatic lapse rate. These data were restored in post processing. However, the user is cautioned that the temperature and humidity data during these seconds after launch are questionable.

b. One sounding failed shortly after launch (16 February 2022, 13:15 UTC) due to a leaking balloon. A second sonde was released 23 minutes later at 13:38 UTC. The data of the failed sounding remain in the set of quality-controlled data and show interesting changes in the lowest 250 m over the span of 20 min.

c. In two soundings the radiosonde failed prior to balloon burst. Sounding 20220108_232857 failed at 10.1 km; and sounding 20220219_081517 failed at 6.7 km.

d. In sounding 20220214_131506, the GPS winds and position measurements were interrupted between 9.17 and 10.03 km. These data were set to missing values.

e. The surface reference observations were entered manually prior to and including the sounding on 13 January. The entered reference pressure values have a small low bias of up to 2 hPa, leading to a few missing profile data points after launch. This was corrected in post processing and missing data were restored from raw data.

The final quality-controlled data are provided in NetCDF format following the CF-1.6 metadata convention for climate and forecasting. For a detailed description of the data format, refer to Vömel et al., 2018, https://doi.org/10.5065/D65X27SR.

5 Sounding metrics

At the CFACT site about 5 km west of Heber City, UT, 120 radiosondes were launched between 7 January and 24 February 2022. Soundings were launched daily at 23:00 UTC and at higher frequency during intensive observation periods.

The distribution of ceiling heights is shown in Figure 2. Burst heights below 16 km occurred randomly on four soundings. In addition to a leaky balloon, two soundings suffered a failure of the temperature sensor and one balloon burst prematurely about 4 km below the average ceiling height. Data were received up to a distance of 187 km. The distribution of balloon distances at ceiling altitude and at 1 km above ground is shown in Figure 3. The median distance at which a sounding was terminated was 72 km and the closest distance was 14 km. At 1 km above ground, the median distance was 0.3 km from the launch site and all balloons were closer than 3.2 km.

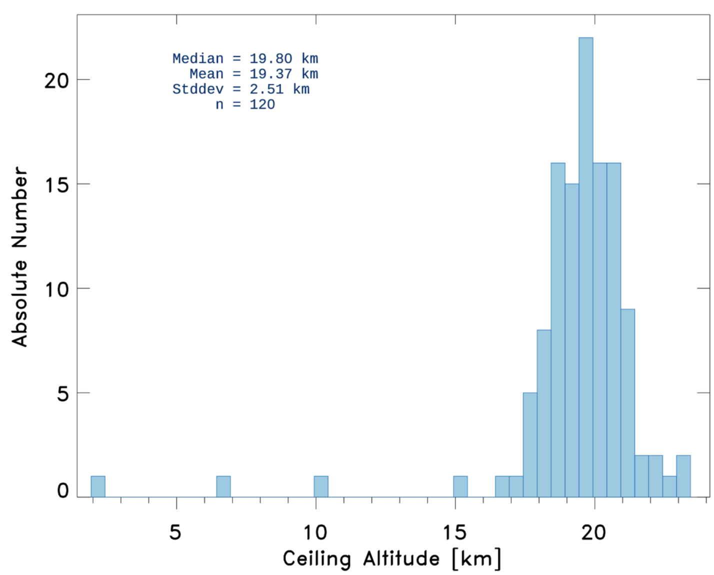

Figure 2: Distribution of ceiling heights for all radiosondes launched during CFACT.

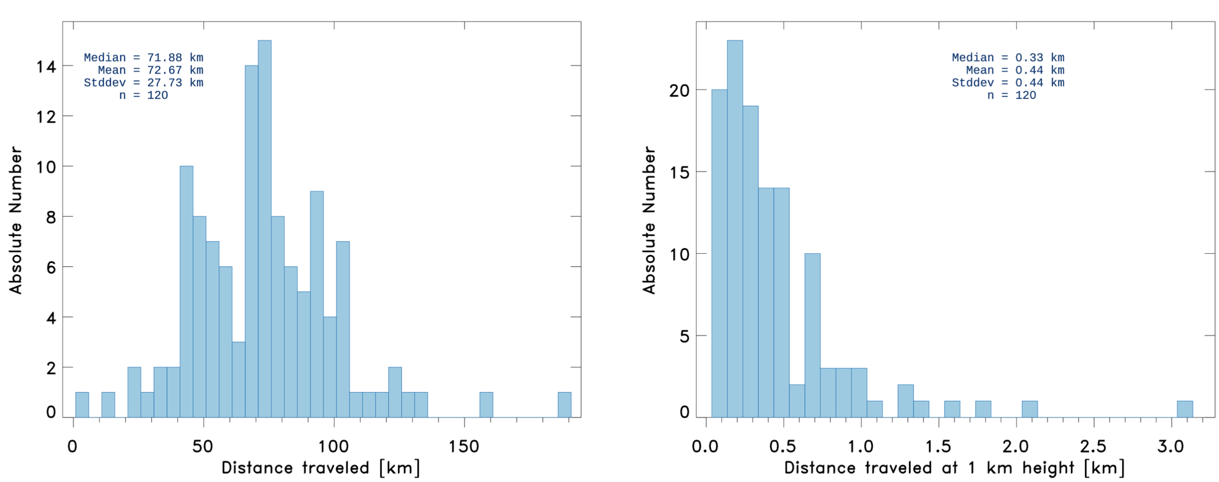

Figure 3: Distribution of balloon distance at end of data recording (left panel) and at 1 km above ground (right panel).

Balloons were typically filled with 20 ft^3 of helium. At the beginning of the campaign, the fill amount was slightly larger with a mean volume of 21.8 ft^3 of helium. The rise rate difference between these fill amounts during CFACT is small. Balloons typically rose with between 3.5 m/s to 4.5 m/s. The profiles of the average rise rate for the two different fill volumes is shown in Figure 4. Sounding 20220210_051501 was underinflated and rose only with an average rate of 2 m/s. Nevertheless, this sounding reached a ceiling altitude of 23.4 km. The distribution of rise rates for all soundings is shown in Figure 5.

The sequence of all balloon rise rates (Figure 6) shows that during CFACT this type of balloon rises faster in the lowest 2 km with an average rise rate of about 4.5 m/s shortly after launch and a minimum of 3.5 m/s at about 4 km altitude. As a result, the vertical resolution of measurements in the lowest troposphere increases from about 4.5 m to 3.5 m between the surface and 4 km altitude.

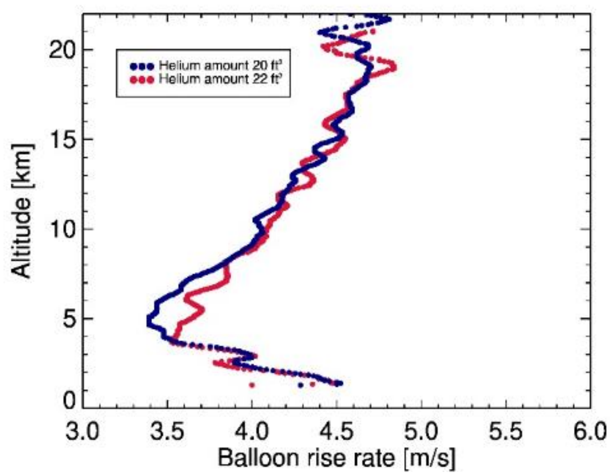

Figure 4: Average rise rates profiles for the two different helium fill values used during CFACT.

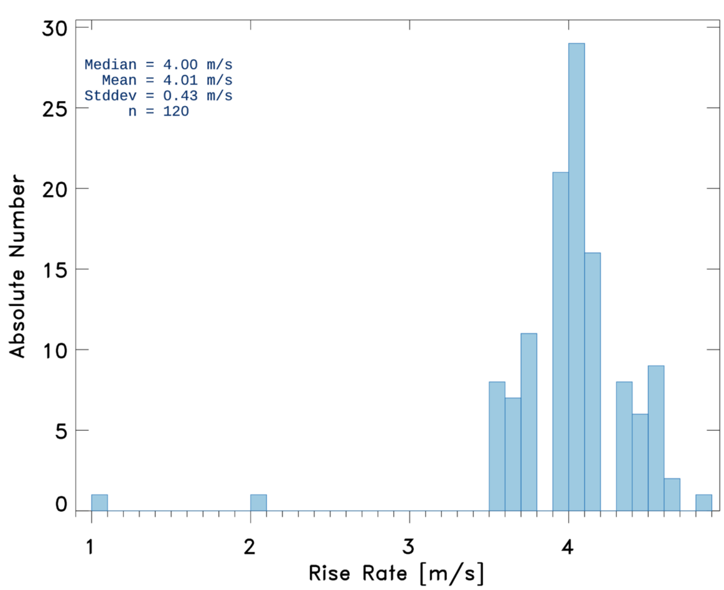

Figure 5: Distribution of rise rates for all radiosondes launched during CFACT.

The maximum rise rate over a 50 m layer was 8.8 m/s and observed only in a few shallow updrafts. No sounding encountered a downdraft.

The underinflated balloon 20220210_051501 only achieved a mean ascent rate of 2.1 m/s but reached the highest ceiling altitude of all balloons at 23.4 km.

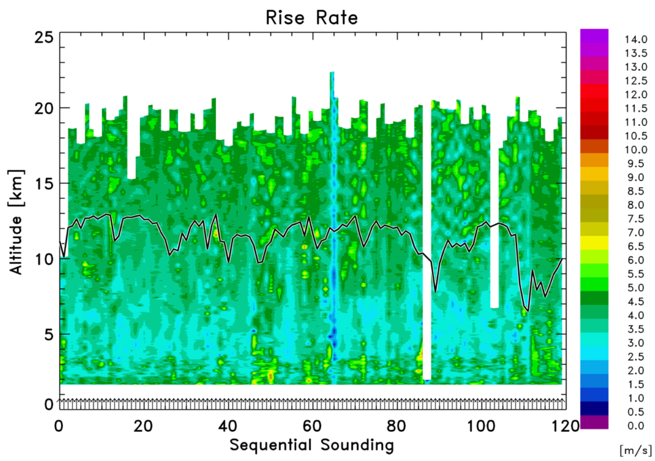

Figure 6: Sequential rise rate profiles as color contours for all radiosondes launched during CFACT. Each launch is indicated by a small arrow at the bottom of the diagram. The intensive observation periods are indicated by the higher density of launch arrows. For a list of all soundings, see Section 7.

6 Atmospheric Measurements

Air temperature and relative humidity measurements from all radiosondes are shown in Figure 7. For most of the project period, the surface temperature during the daytime was above freezing and below during nighttime. During the last three days of the project, all balloons were launched at temperature well below freezing. The tropopause (shown as thin black line) ranged between about 10 and 13 km for most of the project and dropped to below 8 km during the last two weeks. It is also indicated by the rapid drop of relative humidity to values of less than 5%. As is customary, all relative humidity profiles are clipped at 100 % relative humidity over liquid.

Individual balloon launches are indicated by arrows at the bottom of each panel. Intensive observation periods are identified by the higher density of arrows.

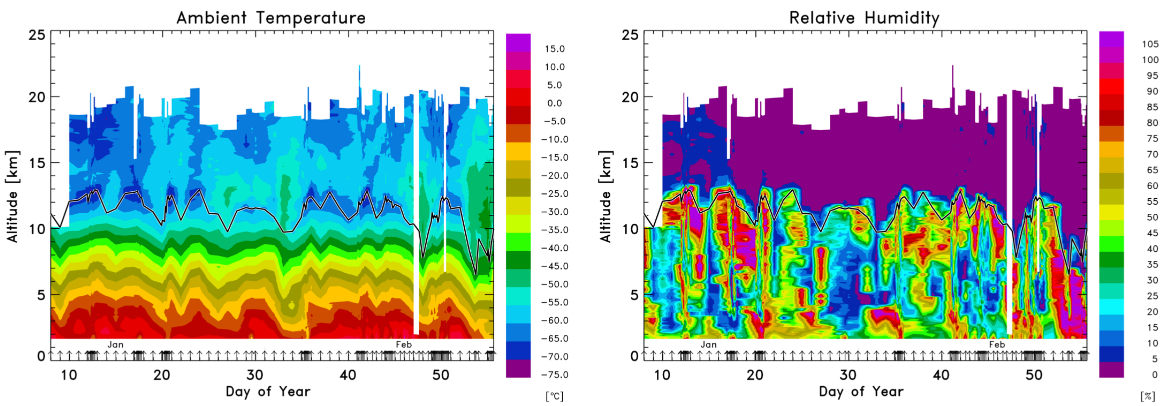

Figure 7: Time series contours of temperature profiles (left) and relative humidity profiles (right) from all radiosondes launched during CFACT. The tropopause is shown as thin black line typically between 10 and 13 km.

The zonal and meridional wind speed measurements are shown in Figure 8. The proximity of the jet stream is indicated by high wind speeds in the upper troposphere reaching up to 57 m/s.

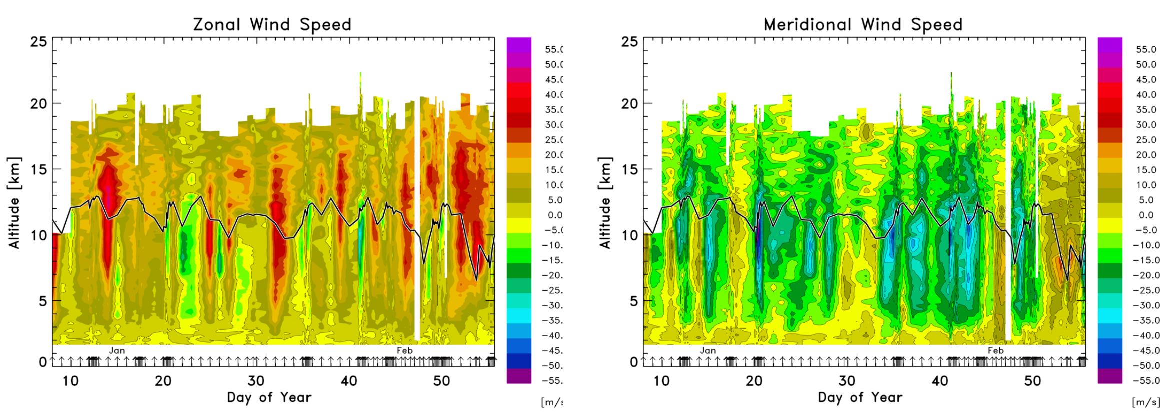

Figure 8: Time series contours of zonal and meridional wind speed profiles for all radiosondes launched during CFACT.

7 List of all soundings

#	Date [UTC]	Time [UTC]	Radiosonde serial number	Ceiling altitude [km]	Rise rate [m/s]	Duration [min]
1	07-Jan-22	23:24:43	N1630290	18.6	3.9	71.8
2	08-Jan-22	23:28:57	M3910679	10.1	4.2	33.5
3	09-Jan-22	23:15:09	N1630292	18.7	3.8	74.1
4	10-Jan-22	23:32:34	N1540198	18.6	3.9	72.9
5	11-Jan-22	21:28:26	N1630289	20.1	4.0	76.3
6	11-Jan-22	23:28:45	N1630291	17.6	3.9	68.4
7	12-Jan-22	05:15:01	T3321958	20.2	4.2	73.2
8	12-Jan-22	07:15:02	T3321956	21.1	4.1	79.8
9	12-Jan-22	09:15:03	T3321951	18.5	4.2	67.7
10	12-Jan-22	11:15:02	T3321959	18.1	4.2	65.2
11	12-Jan-22	14:15:01	T3321957	19.9	4.2	73.3
12	12-Jan-22	17:10:13	T3321945	21.1	3.9	82.6
13	12-Jan-22	23:20:14	M3910680	19.2	4.5	64.2
14	13-Jan-22	23:37:00	T3321952	19.4	4.0	74.9
15	14-Jan-22	23:29:19	T3321954	19.9	3.7	81.2
16	15-Jan-22	23:15:12	T3321942	20.8	3.9	81.1
17	16-Jan-22	21:21:39	T3321941	21.4	4.0	83.2
18	16-Jan-22	23:15:27	T3340490	15.3	3.9	58.7
19	17-Jan-22	05:16:39	T3340487	16.8	3.8	65.3
20	17-Jan-22	07:15:00	T3340498	19.3	3.9	75.5
21	17-Jan-22	09:14:59	T3340484	19.4	3.9	75.6
22	17-Jan-22	11:15:01	T3340482	20.2	4.0	78.0
23	17-Jan-22	14:14:41	T3340481	20.3	4.1	75.7
24	17-Jan-22	17:15:19	T3340480	19.8	4.1	73.1
25	17-Jan-22	23:08:25	T3340469	20.5	3.9	79.8
26	18-Jan-22	23:13:12	T3340470	18.5	4.0	70.7
27	19-Jan-22	21:40:32	T3340216	20.6	4.2	75.5
28	19-Jan-22	23:16:21	T3340228	19.9	4.2	72.0
29	20-Jan-22	05:17:20	T3340201	20.7	3.8	82.6
30	20-Jan-22	07:15:02	T3321955	18.4	4.1	67.2
31	20-Jan-22	09:15:35	T3321946	18.4	4.3	65.5
32	20-Jan-22	11:15:07	T3340213	19.7	3.9	76.8
33	20-Jan-22	14:15:01	T3321948	19.6	4.0	74.3
34	20-Jan-22	17:24:23	T3321953	18.6	4.0	70.0
35	20-Jan-22	23:30:18	T3321939	19.8	4.1	74.5
36	21-Jan-22	23:05:14	T3340214	19.9	3.9	78.8
37	22-Jan-22	23:15:20	T3340485	20.6	3.9	80.5
38	23-Jan-22	23:15:03	T3321961	20.7	4.1	77.3
39	24-Jan-22	23:15:03	T3321949	17.9	4.3	62.4
40	25-Jan-22	23:15:03	T3321950	21.1	4.1	79.9
41	26-Jan-22	23:29:10	T3321947	17.4	4.0	66.3
42	27-Jan-22	23:15:07	T3321960	18.6	4.0	70.1
43	28-Jan-22	23:16:11	T3340492	19.1	4.2	68.8
44	29-Jan-22	14:19:03	T3340476	19.9	4.0	75.2
45	29-Jan-22	23:15:52	T3340475	18.7	4.1	69.8
46	30-Jan-22	23:15:11	T3340486	19.6	3.7	81.4
47	31-Jan-22	23:30:48	T3340477	19.8	3.9	77.3
48	01-Feb-22	23:10:35	T3340548	18.5	4.4	63.0
49	02-Feb-22	23:15:04	T3340559	18.5	4.5	61.9

50	03-Feb-22	21:19:04	T3340547	20.4	4.3	72.9
51	03-Feb-22	23:15:57	T3340538	18.3	4.8	58.0
52	04-Feb-22	05:17:39	T3340537	19.6	4.3	70.0
53	04-Feb-22	07:16:59	T3321996	19.4	4.0	73.2
54	04-Feb-22	09:15:04	T3321692	19.4	4.0	74.8
55	04-Feb-22	11:37:28	T3321691	18.2	3.6	77.4
56	04-Feb-22	14:15:24	T3321687	21.1	3.6	89.2
57	04-Feb-22	17:17:04	T3321988	20.7	4.1	77.5
58	04-Feb-22	23:12:38	T3340562	19.5	4.3	69.4
59	05-Feb-22	23:21:11	T3340560	18.2	4.4	62.7
60	06-Feb-22	23:15:06	T3340561	20.0	4.5	67.3
61	07-Feb-22	23:10:28	T3340409	19.8	4.5	67.3
62	08-Feb-22	23:15:08	T3340549	19.1	4.5	64.7
63	09-Feb-22	21:02:08	T3340536	23.0	4.1	87.5
64	09-Feb-22	23:15:10	T3340552	19.9	4.2	71.6
65	10-Feb-22	02:15:00	T3340551	22.3	3.7	92.6
66	10-Feb-22	05:15:01	T3321690	23.4	2.1	172.1
67	10-Feb-22	08:59:08	T3321689	20.7	3.8	84.4
68	10-Feb-22	11:15:03	T3321684	18.7	4.2	67.0
69	10-Feb-22	14:15:03	T3321688	18.6	3.9	72.6
70	10-Feb-22	17:23:15	T3321997	21.3	4.2	78.0
71	10-Feb-22	23:25:53	T3321683	19.3	4.4	66.2
72	11-Feb-22	13:23:44	T3330606	20.5	4.1	76.0
73	11-Feb-22	23:14:12	T3321992	20.7	4.5	69.9
74	12-Feb-22	13:15:02	T3330604	20.4	3.8	82.3
75	12-Feb-22	21:03:48	T3321888	18.0	3.8	71.6
76	12-Feb-22	23:15:07	T3321885	19.3	4.3	68.4
77	13-Feb-22	02:18:24	T3321991	20.2	4.0	77.6
78	13-Feb-22	05:26:03	T3321928	21.2	3.8	84.6
79	13-Feb-22	08:15:02	T3321990	18.9	4.5	63.4
80	13-Feb-22	11:06:21	T3321987	19.8	4.0	75.1
81	13-Feb-22	14:09:20	T3321685	19.1	4.4	66.2
82	13-Feb-22	17:41:07	T3321894	19.2	4.2	69.5
83	13-Feb-22	23:16:18	T3321893	20.7	4.2	75.3
84	14-Feb-22	13:15:06	T3321889	18.0	3.6	75.3
85	14-Feb-22	23:13:32	T3321887	20.0	3.7	81.6
86	15-Feb-22	13:18:37	N1630287	20.3	4.2	75.0
87	15-Feb-22	23:21:24	N1740046	20.2	4.1	74.6
88	16-Feb-22	13:15:48	N1740047	1.9	1.0	4.4
89	16-Feb-22	13:38:13	N1540195	20.5	4.0	77.9
90	16-Feb-22	23:14:40	N1740045	20.5	3.7	84.9
91	17-Feb-22	13:15:02	N1740044	20.4	3.8	81.7
92	17-Feb-22	21:10:19	T3321874	19.9	3.9	78.1
93	17-Feb-22	23:16:34	T3321881	21.2	3.8	84.9
94	18-Feb-22	02:18:13	T3321926	19.8	3.6	83.6
95	18-Feb-22	05:16:09	T3321883	21.1	3.9	82.5
96	18-Feb-22	08:15:23	T3321876	20.5	3.9	80.3
97	18-Feb-22	11:14:42	T3320562	18.9	3.6	78.9
98	18-Feb-22	14:15:04	T3340625	20.0	3.9	77.6
99	18-Feb-22	17:18:17	T3330269	20.6	4.2	74.5
100	18-Feb-22	21:24:30	T3321880	19.2	4.3	67.7
101	18-Feb-22	23:15:07	T3321886	22.0	3.9	86.3
102	19-Feb-22	02:15:01	N1740038	20.1	3.7	82.8

103	19-Feb-22	05:14:23	N1530430	19.6	3.6	82.5
104	19-Feb-22	08:15:17	N1740042	6.7	3.5	23.6
105	19-Feb-22	11:15:24	N1540200	17.3	3.9	67.4
106	19-Feb-22	14:15:03	N1540193	17.8	4.4	61.8
107	19-Feb-22	17:15:04	N1540300	21.6	3.8	88.4
108	19-Feb-22	23:06:56	N1740039	19.4	3.8	77.2
109	20-Feb-22	23:13:37	N1630294	21.7	4.0	83.6
110	21-Feb-22	23:15:50	N1540201	20.7	4.0	80.1
111	22-Feb-22	13:15:01	N1630293	19.1	3.9	74.3
112	22-Feb-22	16:01:24	T3340488	22.9	3.5	100.6
113	22-Feb-22	23:29:16	T3321993	19.8	4.6	65.8
114	23-Feb-22	21:51:04	T3330270	19.9	4.5	67.5
115	23-Feb-22	23:30:56	T3321878	19.4	4.4	67.7
116	24-Feb-22	02:15:54	N1740040	18.6	4.3	65.0
117	24-Feb-22	05:17:58	N1530453	17.8	4.7	56.8
118	24-Feb-22	08:17:22	N1540197	18.6	4.5	62.7
119	24-Feb-22	11:14:06	T3340608	19.4	4.2	69.8
120	24-Feb-22	14:07:02	N1630284	20.3	3.7	83.6

8 References

Vömel, H., G. Granger, and I. Suhr, 2018, NCAR/EOL/ISF Radiosonde NetCDF Data Files, UCAR/NCAR - Earth Observing Laboratory. https://doi.org/10.5065/D65X27SR.